Available online at www.sciencedirect.com

SciVerse ScienceDirect

Ceramics International 38 (2012) 4895–4900

CERAMICS INTERNATIONAL

www.elsevier.com/locate/ceramint

Synthesis and photoluminescence properties of the high-brightness Eu^{3+}-doped $Sr_3Y(PO_4)_3$ red phosphors

Baozhu Yang, Zhiping Yang, Yufeng Liu *, Fachun Lu, Panlai Li, Yanmin Yang, Xu Li

College of Physics Science and Technology, Hebei University, Baoding 071002, China

Received 7 February 2012; received in revised form 24 February 2012; accepted 24 February 2012
Available online 5 March 2012

Abstract

A series of red-emitting phosphors Eu^{3+}-doped $Sr_3Y(PO_4)_3$ have been successfully synthesized by conventional solid-state reaction, and its photoluminescence properties have been investigated. The excitation spectra reveal strong excitation bands at 392 nm, which match well with the popular emissions from near-UV light-emitting diode chips. The emission spectra of $Sr_3Y(PO_4)_3$:Eu^{3+} phosphors exhibit peaks associated with the $^5D_0 \rightarrow {}^7F_J$ ($J = 0, 1, 2, 3, 4$) transitions of Eu^{3+} and have dominating emission peak at 612 nm under 392 nm excitation. The integral intensity of the emission spectra of $Sr_3Y_{0.94}(PO_4)_3$:$0.06Eu^{3+}$ phosphors excited at 392 nm is about 3.4 times higher than that of Y_2O_3:Eu^{3+} commercial red phosphor. The Commission Internationale de l'Eclairage chromaticity coordinates, the quantum efficiencies and decay times of the phosphors excited under 392 nm are also investigated. The experimental results indicate that the Eu^{3+}-doped $Sr_3Y(PO_4)_3$ phosphors are promising red-emitting phosphors pumped by near-UV light.

Keywords: A. Powders: solid state reaction; C. Optical properties; Luminescence; Phosphors

1. Introduction

In recent years, great progress has been made on white light-emitting diodes (w-LEDs) with high efficiency, long lifetime, energy saving, and environment-friendly characteristics. The most popular approach in fabricating w-LEDs is by coating a yellow emitting phosphor on a blue emitting InGaN LED. Yttrium aluminum garnet doped with cerium (YAG:Ce) is commonly used as the yellow phosphor for this purpose. However, w-LEDs fabricated in this way give bi-chromatic white light with poor color quality (CRI ~ 70) due to lack of red component [1]. One of the most promising approaches to generate white light in w-LEDs is to use a LED emitting near-UV light (near-UVLED, 350–400 nm) coated with blue, green and red tri-color phosphors. This approach yields a more balanced white spectra than the traditional blue emitter + - yellow phosphor [2,3]. Current available commercial phosphors are $BaMgAl_{10}O_{17}$:Eu^{2+} and $(Ca,Sr,Ba)_{10}(PO_4)_6Cl_2$:$Eu^{2+}$ as blue phosphors and $SrGa_2S_4$:Eu^{2+} and $BaMgAl_{10}O_{17}$:(Eu^{2+}, Mn^{2+}) as green phosphors. The red phosphors Y_2O_3:Eu^{3+}, Y_2O_2S:Eu^{3+} and YVO_4:Eu^{3+}, although have strong emissions under the excitation of around 250–330 nm, its absorptions in the region of 370–410 nm are very weak [4]. In addition, current sulfide and oxysulfide as red phosphors suffer chemical instability and decompose at high temperature. Recently, nitrides-based compounds such as $CaAlSiN_3$:Eu^{2+} have been demonstrated to be promising candidate as red phosphors due to their good thermal stability and high luminescence efficiency [5]. However, their synthesis process requires very high firing temperatures and nitrogen pressures, which results in higher production costs. Many researches have been conducted in order to develop new red phosphors suitable for near-UV LED excitations [6,7]. However, up to now, satisfactory red phosphors for the w-LEDs applications are not available.

Trivalent Eu ion is expected to be one of the promising species that provide optical devices in red color regions and many investigations have been conducted in various compounds [8]. Phosphates are a type of promising host materials for their easy-synthesis, low-cost and chemical/thermal-stabilities over a wide range of temperatures. Previous reports indicate that eulytite-type materials can act as eminent matrices for solid state fluorescence because the disordered structure

* Corresponding author. Tel.: +86 312 7546423.
E-mail address: liuyufeng4@126.com (Y. Liu).

0272-8842/$36.00
doi:10.1016/j.ceramint.2012.02.080

contributes to the luminescence [9–15]. It is well known that rare earth doped eulytite-type materials have fairly good luminescence properties, such as $Ba_3Y(PO_4)_3:Eu^{3+}$ [11], $LnSr_3(PO_4)_3:Ln = Ce^{3+}$, Pr^{3+}, Tb^{3+} [12], $LaSr_3(PO_4)_3$: Ce^{3+}, Tb^{3+} [13] and $Sr_3Y_{1-x}(PO_4)_3:xTb^{3+}$ [14]. Since the $Sr_3Y(PO_4)_3:Eu^{3+}$ red phosphors were first synthesized by a modified wet chemical method [15], there are several papers studied the photoluminescence (PL) properties of $Sr_3Y(PO_4)_3:Eu^{3+}$. In this paper, $Sr_3Y_{1-x}(PO_4)_3:xEu^{3+}$ red-emitting powders were synthesized by a conventional solid-state reaction, and its PL properties were investigated in detail. The potential applications for the red component of w-LEDs phosphors are discussed by comparing with $Y_2O_3:Eu^{3+}$.

2. Experimental

A series of microcrystalline powders of $Sr_3Y_{1-x}(PO_4)_3:xEu^{3+}$ ($0.005 \leq x \leq 0.10$) were prepared by solid-state reactions. Raw materials used in the experiment were $SrCO_3$ (≥99.9%), Y_2O_3 (≥99.9%), $NH_4H_2PO_4$ (≥99.9%) and Eu_2O_3 (99.99%). The raw materials with stoichiometrical ratio were weighed and mixed in mortar. In order to obtain the target compound with pure phase, two firing steps were necessary. The mixture was firstly heated at 900 °C for 2 h in a covered alumina crucible, then reground thoroughly after cooled down to the room temperature. The second firing was conducted at 1200 °C for 8 h. The final products were obtained by cooling down to room temperature in the furnace.

The powder sample was characterized using powder X-ray diffraction (XRD) in a Bruker AXS D8 advanced automatic diffractometer (Bruker Co., Germany) with Ni-filtered Cu $K_{\alpha 1}$ radiation (λ = 1.5406 Å). PL excitation and emissions spectra were measured in a fluorescence spectrophotometer (Hitachi F-4600). The chromaticity data were taken by using the PMS-80 spectra analysis system. Spectra for the quantum yield measurement were collected using an integrated sphere. Powder samples were mixed with appropriate methanol, spread over a quartz plate, dried at ambient atmosphere, and mounted inside the sample chamber of the integrated sphere. Lifetime measurement for Eu^{3+} transitions was carried out using μs flash lamp attached to Edinburgh Instruments (model FLS 920). All the measurements were conducted at room temperatures.

3. Results and discussion

3.1. Phase characterization

The crystal structures of the eulytite-type materials $A_3M(PO_4)_3$ (A = Ca, Sr, Ba, M = La–Lu, Y) are well known to be cubic (space group number 220) and isomorphous with eulytine mineral ($Bi_4Si_3O_{12}$) [6]. The A^{2+}/M^{3+} pairs of cations are disordered on a single crystallographic site whilst the oxygen atoms of the phosphate groups are distributed over three partially occupied sites [5]. The Eu^{3+} dopant ions substitute in the single disordered cationic sites having C_3 point group symmetry.

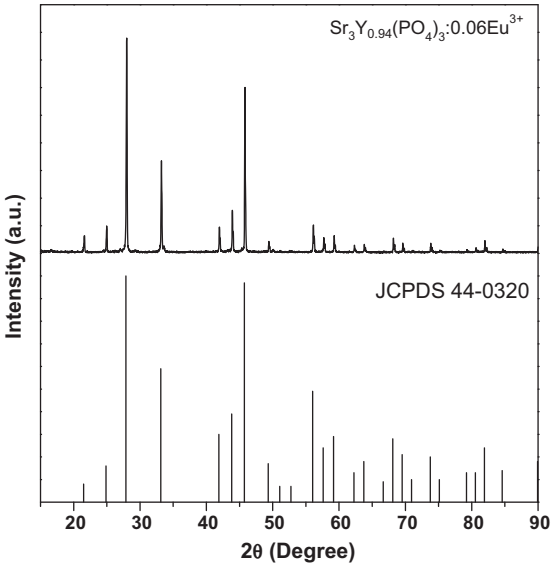

Fig. 1. The XRD patterns of JCPDS file No. 44-0320 and $Sr_3Y_{0.94}(PO_4)_3:0.06Eu^{3+}$.

The XRD patterns of JCPDS file No. 44-0320 and $Sr_3Y_{0.94}(PO_4)_3:0.06Eu^{3+}$ are shown in Fig. 1. It was found to be consistent with that reported in JCPDS file No. 44-0320. The XRD analysis was performed to determine the chemical purity and phase homogeneity of the $Sr_3Y_{0.94}(PO_4)_3:0.06Eu^{3+}$ phosphor. The lattice parameters of $Sr_3Y_{0.94}(PO_4)_3:0.06Eu^{3+}$ phases were calculated based on the experimental XRD profiles with cell refinement software. The lattice parameters of $Sr_3Y(PO_4)_3$ powder were found to be $a = b = c = 10.1091$ Å, $Z = 4$ and $V = 1033.09$ Å^3. As Y^{3+} was substituted by a larger Eu^{3+} ion in $Sr_3Y(PO_4)_3$ host, the lattice parameters of $Sr_3Y_{0.94}(PO_4)_3:0.06Eu^{3+}$ became $a = b = c = 10.1105$ Å, $V = 1033.52$ Å^3. The cell parameters do not appear to be significantly affected by the nature of the Eu^{3+} ion. These results indicated that Eu^{3+} ions were undoubtedly doped into and entered the $Sr_3Y(PO_4)_3$ crystal lattice.

3.2. Photoluminescence properties of $Sr_3Y(PO_4)_3:Eu^{3+}$

The $Sr_3Y(PO_4)_3$ compound has the structural type of eulytine, and Y^{3+} ion occupies a distorted octahedron of oxygen ions due to three short and three long Y–O distances. Therefore, we can predict that Y^{3+} ions occupy noninversion centrosymmetric sites. We also assume that Y^{3+} ions are replaced by Eu^{3+} ions in $Sr_3Y(PO_4)_3:Eu^{3+}$ because they have the same valence and ionic radii. So, a red emission ($^5D_0 \rightarrow {}^7F_2$) whose intensity is stronger than that of the orange emission ($^5D_0 \rightarrow {}^7F_1$) could be obtained from $Sr_3Y_{1-x}(PO_4)_3:xEu^{3+}$ phosphors.

The fluorescence excitation spectra of typical sample $Sr_3Y_{0.94}(PO_4)_3:0.06Eu^{3+}$ monitoring at the $^5D_0 \rightarrow {}^7F_2$ emission (613 nm) were shown in Fig. 2(a). The excitation spectra of Eu^{3+} doped $Sr_3Y(PO_4)_3$ clearly indicate a broad absorption from 220 to 310 nm (with a maximum at about 270 nm) and several excitation bands located at 318 nm ($^7F_{0,1} \rightarrow {}^5H_{3,6}$), 360 nm ($^7F_{0,1} \rightarrow {}^5D_4$), 380 nm ($^7F_{0,1} \rightarrow {}^5L_7$), 392 nm

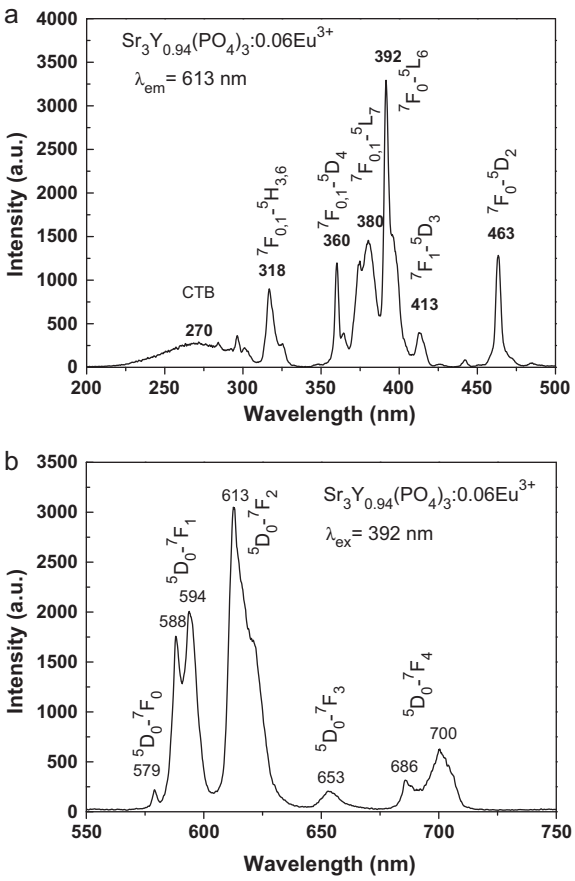

Fig. 2. Excitation and emission spectra of $Sr_3Y_{0.94}(PO_4)_3$:0.06Eu^{3+} (a: λ_{em} = 613 nm, b: λ_{ex} = 392 nm).

($^7F_0 \rightarrow {}^5L_6$), 413 nm ($^7F_1 \rightarrow {}^5D_3$), 463 nm ($^7F_0 \rightarrow {}^5D_2$) [11], respectively. The broad absorption from 220 to 310 nm can be attributed to charge-transfer transition from negative oxygen ion ($2p^6$) to the empty state of $4f^7$ of Eu^{3+} ion [ligand-to-metal charge-transfer band (CTB)] [16]. The strongest absorption band of $^7F_0 \rightarrow {}^5L_6$ transition at 392 nm matches well with the output wavelength of near-UV chips in phosphor-converted w-LEDs. Another strong excitation peak in the blue region is located at 463 nm, whose intensity is inferior to that of 392 nm.

The emission spectra of $Sr_3Y_{0.94}(PO_4)_3$:0.06Eu^{3+} phosphors under 380, 463 nm (not shown) and 392 nm excitation show the same position of emission peaks, except for the intensity. The emission intensity under the 380 or 463 nm excitation is remarkably lower than that of 392 nm because of the relatively lower absorption at this wavelength (Fig. 2(a)). Fig. 2(b) illustrates the PL spectra of $Sr_3Y_{0.94}(PO_4)_3$:0.06Eu^{3+} phosphor excited at 392 nm. The bands with the maxima at 579, 588, 594, 613, 653, 686 and 700 nm of $Sr_3Y_{0.94}(PO_4)_3$:0.06Eu^{3+} phosphor are assigned to the $^5D_0 \rightarrow {}^7F_J$ (J = 0, 1, 2, 3, 4) transition of Eu^{3+}, respectively [11]. In addition, from the emission spectra, the red emission ($^5D_0 \rightarrow {}^7F_2$) is stronger than the orange emission ($^5D_0 \rightarrow {}^7F_1$), indicating that Eu^{3+} is located in a noncentrosymmetric position in the $Sr_3Y(PO_4)_3$ matrix, which agrees with the conclusion of the structural analysis.

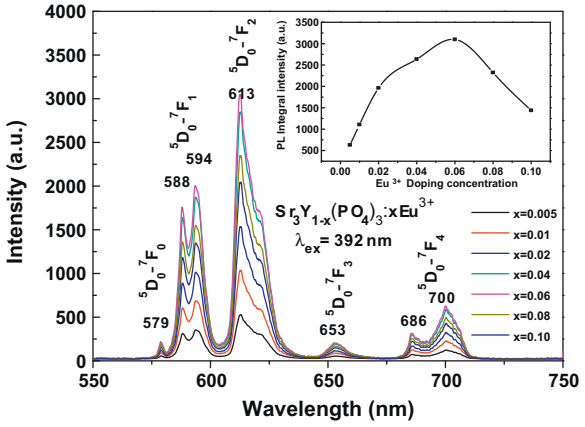

Fig. 3. The emission spectrum of $Sr_3Y_{1-x}(PO_4)_3$:xEu^{3+} ($0.005 \leq x \leq 0.10$, λ_{ex} = 392 nm). The inset presents the integral intensity versus Eu^{3+} concentration from 550 nm to 750 nm.

In order to obtain the best doping concentration of Eu^{3+}, a series of $Sr_3Y_{1-x}(PO_4)_3$:xEu^{3+} ($0.005 \leq x \leq 0.10$) phosphors have been prepared. Fig. 3 presents the $^5D_0 \rightarrow {}^7F_2$ emission intensity as a function of Eu^{3+} concentration in $Sr_3Y(PO_4)_3$:Eu^{3+} phosphor. From Fig. 3, it can be seen that all the profiles of the emission spectra of $Sr_3Y_{1-x}(PO_4)_3$:xEu^{3+} are similar under the excitation of 392 nm, whereas the intensity increases initially with Eu^{3+} concentration, and after reaching a maximum value, it decreases with the further increase of Eu^{3+} concentration. This phenomenon can be readily explained by concentration quenching effect. When Eu^{3+} concentration is low, the interaction of Eu^{3+}–Eu^{3+} can be almost neglected and the emission intensity increases with Eu^{3+} concentration. With the further increase of Eu^{3+} concentration, the enhanced nonradiative energy transfer between Eu^{3+} ions will finally decrease the fluorescence emission. The inset of Fig. 3 presents the integral intensity versus Eu^{3+} concentration from 550 nm to 750 nm. From that, the quenching concentration is found at about x = 0.06 of Eu^{3+} content.

While discussing the mechanism of energy transfer in phosphors, it is necessary to obtain the critical distance (R_c), i.e. the critical separation between the donor (activator) and acceptor (quenching site). Blasse suggested that the R_c of energy transfer can be calculated by the critical concentration of the activator ion [17]. The critical distance between Eu^{3+} ions for energy transfer can be calculated using the relation proposed by Blasse [18]

$$R_c \approx 2\left[\frac{3V}{4\pi x_c N}\right]^{1/3} \quad (1)$$

where V is the volume of the unit cell, x_c is the critical concentration of the activator ion, and N is the number of host cations in the unit cell. For the $Sr_3Y(PO_4)_3$ host, by taking the values of N = 4 ($N = Z \times 1$, Z is the number of formula per unit cell), x_c = 0.06, and V = 1033.52 Å^3, the obtained R_c value is 20.19 Å.

Non-radiative energy transfer between different Eu^{3+} ions in the luminescence of oxidic phosphors may occur by radiation

re-absorption, exchange interaction, or multipole–multipole interaction. Generally speaking, the mechanism of radiation re-absorption comes into effect only when there is a broad overlap of the fluorescent spectra of the sensitizer and activator, and in view of the emission and excitation spectra of $Sr_3Y(PO_4)_3$:Eu^{3+} phosphor, the radiation re-absorption is unlikely to be occurring in this case. The mechanism of exchange interaction plays the role in energy transfer both when the overlapping of the wave functions of the sensitizer and activator is enough to exchange electronics and when the activator and sensitizer occupy adjacent lattice sites. Eu^{3+} is an isolated emission center in $Sr_3Y(PO_4)_3$:Eu^{3+} phosphor and typical critical distance is then about 5 Å [17], which is far less than that of the sated calculation result of Eu^{3+}-doped in $Sr_3Y(PO_4)_3$. This indicates that the mechanism of exchange interaction plays little role in energy transfer between Eu^{3+} ions in $Sr_3Y(PO_4)_3$:Eu^{3+} phosphor. In short, the situation in Eu^{3+} compounds can be characterized as follows: [16] if the Eu^{3+}–Eu^{3+} distance is shorter than 5 Å, the exchange interaction becomes effective, if the Eu^{3+}–Eu^{3+} distance is larger than 5 Å, the exchange interaction becomes ineffective, and only a multipolar interaction is important. As the R_c of Eu^{3+}–Eu^{3+} for the $Sr_3Y(PO_4)_3$:Eu^{3+} phosphor is calculated to be 20.19 Å, the multipolar interaction is the dominant mechanism of concentration quenching of Eu^{3+} in the $Sr_3Y(PO_4)_3$:Eu^{3+} phosphor. In addition, it is well known that the $^5D_0 \rightarrow {}^7F_2$ transition of Eu^{3+} is an electric–dipole transition, so the process of energy transfer should be controlled by electric multipole–multipole interaction according to Dexter's theory [19].

When the electric multipolar interaction is involved in the energy transfer, there are several types of interactions [such as dipole–dipole (d–d), dipole–quadrupole (d–q), quadrupole–quadrupole (q–q) interactions, and so on]. It is necessary to elucidate which type of interaction is involved in the energy transfer. According to Vanuitert's study that if the energy transfer occurs among the same sorts of activators, the strength of the multipolar interaction can be determined from the change of the emission intensity level which has the multipolar interaction [20]. The emission intensity (I) per activator ion follows the equation [20]:

$$\frac{I}{x} = k[1 + \beta(x)^{\theta/3}]^{-1} \quad (2)$$

where I is the integral intensity of emission spectra from 550 nm to 750 nm, x is the activator concentration, I/x is the emission intensity (I) per activator (x). K and β are constants for a given host under the same excitation condition. According to Eq. (2), $\theta = 3$ for the energy transfer among the nearest-neighbor ions (exchange interaction), while $\theta = 6$, 8, and 10 for d–d, d–q, and q–q interactions, respectively [20]. Assuming that $\beta(x)^{\theta/3} \gg 1$, Eq. (2) can be simplified as follow: [21]

$$\log\frac{I}{x} = K' - \frac{\theta}{3}\log x \quad (K' = \log K - \log\beta) \quad (3)$$

From Eq. (3), the electric multipolar character θ can be obtained by the slope ($-\theta/3$) of the plot $\log(I/x)$ vs. $\log(x)$.

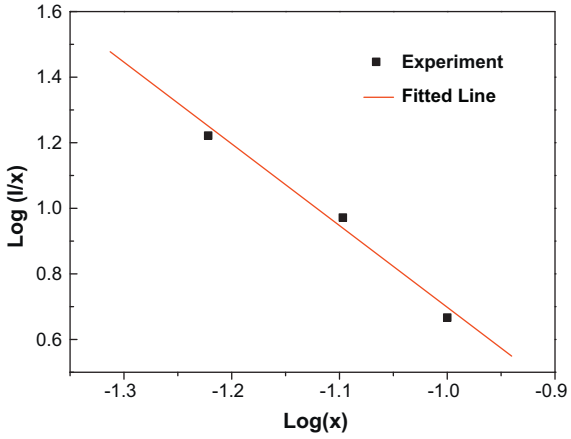

Fig. 4. The relationship of $\log(I/x)$ vs. $\log(x)$ in $Sr_3Y_{1-x}(PO_4)_3$:xEu^{3+} phosphor.

Since the critical concentration of Eu^{3+} can be estimated as 6 mol% from the inset of Fig. 3, the dependence of the emission intensity on the doped-Eu^{3+} concentration based on Fig. 3 for concentration greater than the critical concentration ($x \geq 0.06$) is determined and it is shown in Fig. 4. Obviously, an approximately linear relation between $\log(I/x)$ and $\log(x)$ can be found, which slope is about -2.50. The θ value can be calculated as 7.50 based on the linear fitting using Eq. (3), which is close to 8. This value indicates that the d–q interaction is the major mechanism for concentration quenching of fluorescence emission for Eu^{3+} ions in $Sr_3Y(PO_4)_3$:Eu^{3+}.

The Y_2O_3:Eu^{3+} commercial red phosphors were used as a reference to investigate the PL properties of $Sr_3Y(PO_4)_3$:Eu^{3+} phosphors. Fig. 5 illustrates the PL excitation emission spectra of $Sr_3Y_{0.94}(PO_4)_3$:$0.06Eu^{3+}$ phosphor excited at 392 nm and Y_2O_3:Eu^{3+} commercial red phosphor excited at 262 and 392 nm. The data were acquired under similar conditions. Comparing the two excitation spectra of $Sr_3Y(PO_4)_3$:Eu^{3+} and Y_2O_3:Eu^{3+} from Fig. 5(a), it can be seen that the overall profiles are similar. Whereas the intensity ratio of Eu^{3+}–O^{2-} CTB to the 4f-4f transition of Eu^{3+} is different. The Y_2O_3:Eu^{3+} shows stronger CTB excitation (from 220 nm to 300 nm) than $Sr_3Y_{0.94}(PO_4)_3$:$0.06Eu^{3+}$, whereas $Sr_3Y_{0.94}(PO_4)_3$:$0.06Eu^{3+}$ shows stronger near-UV excitation (from 350 nm to 400 nm) and blue excitation (463 nm). As well known, the resonant excitations of 4f-4f transitions for trivalent rare earth ions are generally weak for they are parity forbidden under the selection rules. So the excitation intensity of CTB should be more intense than that of 4f-4f transitions. However, the opposite situation is observed here, which is believed to be associated with effective charge [22]. In our case the effective charge could be induced via a small amount of Eu^{3+} institute Sr^{2+} sites for Y^{3+} and Sr^{2+} sharing the same sites. The positive effective charge gives rise to a considerable nonradiative loss in the excited state of the Eu^{3+} ion, so the Eu^{3+} complex undergoes an expansion in the excited charge-transfer state, which causes the intensity of 4f-4f transitions more intense than that of the charge transfer band. The strong excitation bands located at 463 nm and 392 nm makes it very attractive for applications such as the red

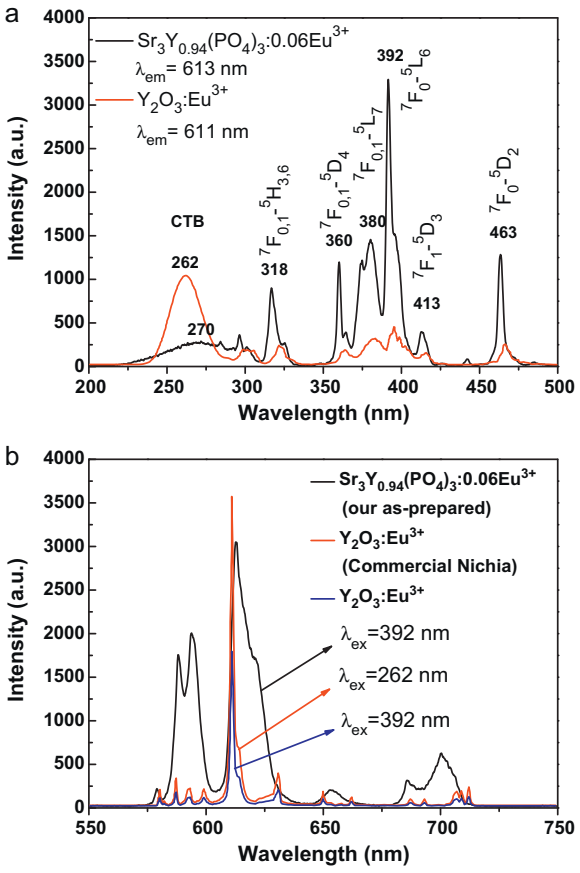

Fig. 5. (a) Excitation spectra of $Sr_3Y_{0.94}(PO_4)_3$:0.06Eu^{3+} (λ_{em} = 613 nm) and commercial Y_2O_3:Eu^{3+} (λ_{em} = 611 nm). (b) Emission spectra of $Sr_3Y_{0.94}(PO_4)_3$:0.06Eu^{3+} (λ_{ex} = 392 nm) and commercial Y_2O_3:Eu^{3+} (λ_{ex} = 262 nm and 392 nm).

component of tricolor luminescence materials, phosphor liquid crystal displays and white lighting devices utilizing GaN-based excitation in the near UV or blue LED chips.

The profiles of emission spectra between our as-prepared and commercial red phosphors Y_2O_3:Eu^{3+} are different too. From Fig. 5(b), It can be seen that the latter has the highest $^5D_0 \rightarrow {}^7F_2$ emission intensity at 611 nm, whereas the peaks of $Sr_3Y_{0.94}(PO_4)_3$:0.06Eu^{3+} phosphor are broader than those of Y_2O_3:Eu^{3+} phosphor and has the highest $^5D_0 \rightarrow {}^7F_2$ emission intensity at 613 nm. The similar phenomenon and explanation can also be found in Ref. [11]. As a result, the integral intensity of the emission spectra for $Sr_3Y_{0.94}(PO_4)_3$:0.06Eu^{3+} phosphor excited at 392 nm is about 3.4 times stronger than that of Y_2O_3:Eu^{3+} excited at 262 nm and 7.5 times stronger than that excited at 392 nm. Therefore, $Sr_3Y(PO_4)_3$:Eu^{3+} phosphor demonstrates high-brightness and might be a good red phosphor candidate for w-LEDs.

3.3. Chromaticity coordinates and quantum efficiency of $Sr_3Y_{0.94}(PO_4)_3$:0.06Eu^{3+}

Under 392 nm excitation, the Commission Internationale de l'Eclairage (CIE) chromaticity coordinates of $Sr_3Y_{0.94}(PO_4)_3$:0.06Eu^{3+} phosphors are (0.64, 0.33), which are very close to the NTSC (National television System Committee)

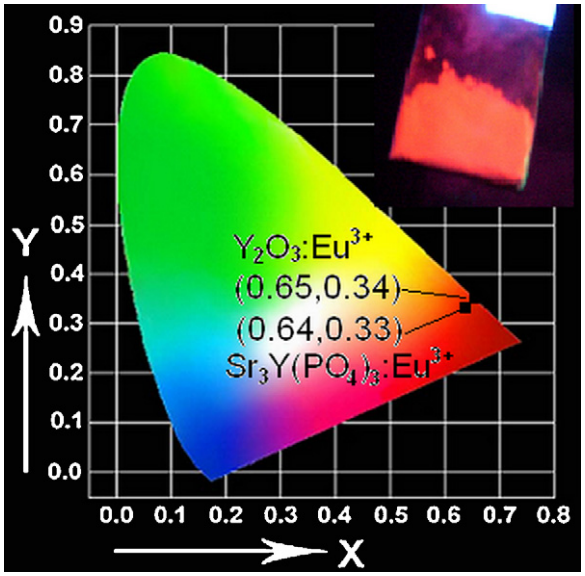

Fig. 6. The CIE chromaticity coordinates of $Sr_3Y_{0.94}(PO_4)_3$:0.06Eu^{3+} and Y_2O_3: Eu^{3+} phosphors.

system standard red chromaticity (0.67, 0.33). It indicates the high color purity of the red phosphors. These chromaticity coordinates are also better than that of the commercially available Y_2O_3:Eu^{3+} (0.65, 0.34) and Y_2O_2S:Eu^{3+} (0.62, 0.34) red phosphors (As shown in Fig. 6). Furthermore, according to their excitation spectra, the $Sr_3Y(PO_4)_3$:Eu^{3+} phosphors can absorb not only the emission of near-UVLED but also that of blue LED. Thus, they can be used to compensate the red color deficiency of YAG:Ce^{3+} or create white light by combining with a blue chip and an other green phosphors.

For photoluminescent applications, the quantum efficiency of a phosphor is often regarded as a measure of its figure of merit. Quantum efficiencies of the selected samples $Sr_3Y_{0.94}(PO_4)_3$:0.06Eu^{3+} were calculated by the method described by De Mello et al. [23] and Palsson and Monkman [24]. Briefly, the method allows determining the sample quantum efficiency Φ_f by measuring the ratio between the number of photons emitted (N_{em}) and the number of those absorbed (N_{ab}) by the sample using the relation: $\Phi_f = N_{em}/N_{ab} = (E_c - E_a)/(L_a - L_c)$, where E_c is the integrated luminescence of the sample caused by direct excitation, E_a is the integrated luminescence from an empty integrating sphere (without the sample, only a blank), L_a is the integrated excitation profile from an empty integrating sphere, and L_c is the integrated excitation profile when the sample is directly excited by the incident beam. The quantum efficiencies for the $Sr_3Y_{0.94}(PO_4)_3$:0.06Eu^{3+} phosphor with 392 nm excitation were calculated by integrating emission counts from the 550 to 750 nm wavelength range. The value is found to be about 75%. Thus, the $Sr_3Y_{0.94}(PO_4)_3$:0.06Eu^{3+} phosphor demonstrates a high quantum efficiency.

3.4. Decay curves for $^5D_0$ level of Eu^{3+} for $Sr_3Y_{0.94}(PO_4)_3$:0.06Eu^{3+} phosphor

The decay curves for $^5D_0$ level of Eu^{3+} for $Sr_3Y_{0.94}(PO_4)_3$:0.06Eu^{3+} are shown in Fig. 7. Excitation wavelength was

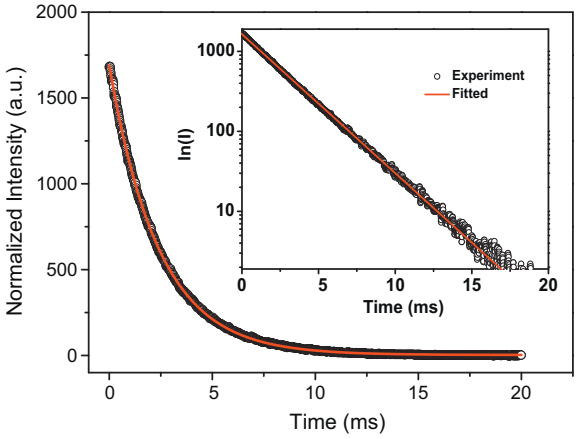

Fig. 7. The decay curves for $^5D_0 \rightarrow {}^7F_1$ of Eu^{3+} of $Sr_3Y_{0.94}(PO_4)_3$:0.06Eu^{3+} under excitation of 392 nm. Inset shows ln(*I*) vs. *t*.

chosen at 392 nm and emission wavelength was fixed at 613 nm. For single exponential decay, it can be expressed as:

$$I = I_0 \exp\left(\frac{-t}{\tau}\right) \quad (4)$$

where I_0 and I are intensities at zero time and time t, respectively, and τ is the lifetime for transition. By taking logarithm, Eq. (4) can be written as

$$\ln(I) = \ln(I_0) - \frac{t}{\tau} \quad (5)$$

The decay data are fitted linearly and are found to follow single exponential decay for $Sr_3Y_{0.94}(PO_4)_3$:0.06Eu^{3+} sample. Typical plot of ln(*I*) vs. *t* for $Sr_3Y_{0.94}(PO_4)_3$:0.06Eu^{3+} is shown in the inset of Fig. 7. From the slope of plot, the lifetime (τ) for transition is calculated, and that is found to be about 2.4 ms. The fluorescence lifetime is short enough for potential applications in w-LEDs.

4. Conclusions

Luminescent material $Sr_3Y(PO_4)_3$:Eu^{3+} were successfully fabricated by using high temperature solid-state reaction at 1200 °C. Its integral emission intensity excited at 392 nm is about 3.4 (or 7.5) times stronger than that of Y_2O_3:Eu^{3+} commercial red phosphor excited at 262 nm (or 392 nm). The CIE chromaticity coordinates and quantum efficiency value of $Sr_3Y(PO_4)_3$:Eu^{3+} phosphor are (0.64, 0.33) and 75%, respectively. The PL properties, good color saturation and the high quantum efficiency indicate that $Sr_3Y(PO_4)_3$:Eu^{3+} phosphors are promising candidate for w-LEDs.

Acknowledgments

This work was financially supported by the National Natural Science Foundation of China (Grant No. 50902042) and the Science and Technology Project of Hebei Province (Grant No. F2009000217).

References

[1] Y.H. Song, G. Jia, M. Yang, Y.J. Huang, H.P. You, H.J. Zhang, $Sr_3Al_2O_5Cl_2$:Ce^{3+},Eu^{2+}: a potential tunable yellow-to-white-emitting phosphor for ultraviolet light emitting diodes, Appl. Phys. Lett. 94 (2009) 901902.
[2] L.Y. Zhou, J.S. Wei, J.R. Wu, F.Z. Gong, L.H. Yi, J.L. Huang, Potential red-emitting phosphor for white LED solid-state lighting, J. Alloys Compd. 476 (2009) 390–392.
[3] C.H. Liang, Y.C. Chang, Y.S. Chang, Synthesis and photoluminescence characteristics of color-tunable BaY_2ZnO_5:Eu^{3+} phosphors, Appl. Phys. Lett. 93 (2008) 211902.
[4] J.G. Wang, X.P. Jing, C.H. Yan, J.H. Lin, F.H. Liao, Influence of fluoride on f-f transitions of Eu^{3+} in $LiEuM_2O_8$ (M = Mo, W), J. Lumin. 121 (2006) 57–61.
[5] J.W. Li, T. Watanabe, N. Sakamoto, H. Wada, O. Setoyama, M. Yoshimura, Synthesis of a multinary nitride, Eu-doped $CaAlSiN_3$, from alloy at low temperatures, Chem. Mater. 20 (6) (2008) 2095–2105.
[6] V.R. Bandi, M. Jayasimhadri, J. Jeong, K. Jang, H.S. Lee, S.S. Yi, J.H. Jeong, Host sensitized novel red phosphor $CaZrSi_2O_7$:Eu^{3+} for near UV and blue LED based White LEDs, J. Phys. D: Appl. Phys. 43 (2010) 395103.
[7] A. Xie, X.M. Yuan, F.X. Wang, Y. Shi, Z.F. Mu, Enhanced red emission in $ZnMoO_4$:Eu^{3+} by charge compensation, J. Phys. D: Appl. Phys. 43 (2010) 055101.
[8] G. Feng, W.H. Jiang, Y.B. Chen, R.J. Zeng, A novel red phosphor $NaLa_4(SiO_4)_3F$ Eu^{3+}, Mater. Lett. 65 (2011) 110–112.
[9] X.Z. Xiao, S. Xu, B. Yan, Photoluminescent properties of Eu^{3+}, Tb^{3+} activated $M_3Ln(PO_4)_3$ (M = Sr, Ca; Ln = Y, La, Gd) phosphors derived from hybrid precursors, J. Alloys Compd. 429 (2007) 255–259.
[10] M.F. Hoogendorp, W.J. Schipper, G. Blasse, Cerium(III) luminescence and disorder in the eulytite structure, J. Alloys Compd. 205 (1994) 249–251.
[11] S.Y. Xin, Y.H. Wang, Z.F. Wang, F. Zhang, Y. Wen, G. Zhu, An intense red-emitting phosphor $YBa_3(PO_4)_3$:Eu^{3+} for near-ultraviolet light emitting diodes application, Electrochem. Solid-State Lett. 14 (11) (2011) H438–H441.
[12] H.B. Liang, Y. Tao, J.H. Xu, H. He, H. Wu, W.X. Chen, S.B. Wang, Q. Su, Photoluminescence of Ce^{3+}, Pr^{3+} and Tb^{3+} activated $Sr_3Ln(PO_4)_3$ under VUV-UV excitation, J. Solid State Chem. 177 (2004) 901–908.
[13] T.W. Kuo, T.M. Chen, A green-emitting phosphor $Sr_3La(PO_4)_3$:Ce^{3+},Tb^{3+} with efficient energy transfer for fluorescent lamp, J. Electrochem. Soc. 157 (2010) J216–J220.
[14] V.B. Taxak, S.D. Han, M. Kumar, S.P. Khatkar, Synthesis and photoluminescence characteristics of $Sr_3Y_{1-x}(PO_4)_3$:xTb^{3+} nanoparticles, ECS Trans. 28 (2010) 115–119.
[15] S. Xu, X.Z. Xiao, B. Yan, Hybrid precursors synthesis and photoluminescence of rare earth ions-activated $Sr_3Y(PO_4)_3$ phosphors, J. Optoelectron. Adv. Mater. 10 (2008) 2727–2731.
[16] G. Blasse, B.C. Grabmaier, Luminescent Materials, vol. 13, Springer-Verlag, Berlin, Germany, 1994.
[17] G. Blasse, Energy transfer in oxidic phosphors, Philips Res. Rep. 24 (1969) 131–144.
[18] G. Blasse, Energy transfer between inequivalent Eu^{2+} ions, J. Solid State Chem. 62 (1986) 207–211.
[19] D.L. Dexter, A theory of sensitized luminescence in solids, J. Chem. Phys. 21 (1953) 836–850.
[20] L.G. Vanuitert, Characterization of energy transfer interactions between rare earth ions, J. Electrochem. Soc. 114 (1967) 1048–1053.
[21] H.Y. Du, J.F. Sun, Z.G. Xia, J.Y. Sun, Luminescence properties of $Ba_2Mg(BO_3)_2$:Eu^{2+} red phosphors synthesized by a microwave-assisted sol–gel route, J. Electrochem. Soc. 156 (12) (2009) J361–J366.
[22] D. Van Voort, G. Blasse, Luminescence of the Eu^{3+} ion in Zr^{4+} compounds, J. Chem. Mater. 3 (6) (1991) 1041–1045.
[23] J.C. De Mello, H.F. Wittmann, R.H. Friend, An improved experimental determination of external photoluminescence quantum efficiency, Adv. Mater. 9 (1997) 230–232.
[24] L.O. Palsson, A.P. Monkman, Measurements of solid-state photoluminescence quantum yields of films using a fluorimeter, Adv. Mater. 14 (2002) 757–758.